PHYSICAL REVIEW C VOLUME 23, NUMBER 2 FEBRUARY 1981

Woods-Saxon potential parameters optimized to the high spin spectra in the lead region

J. Dudek
Kernfysisch Versneller Instituut, Groningen University, Groningen, The Netherlands and Institute of Theoretical Physics, Warsaw University, Warsaw, Poland

Z. Szymański and T. Werner
Institute of Theoretical Physics, Warsaw University, and Institute for Nuclear Research, Warsaw, Poland

(Received 5 June 1980)

The parametrization of the spin-orbit part of the Woods-Saxon potential was optimized taking into account the single-particle energies corrected for nucleon-nucleus interaction and the high-spin spectra of ^{204}Pb and ^{212}Rn. With the spin-orbit potential strength parameters $\lambda = 36.0$ and the radius parameter $(r_0)_{so} = 1.3$ fm for both protons and neutrons, both types of empirical data are reproduced well. The configurations of the calculated high-spin states are identical with the shell-model results.

[NUCLEAR STRUCTURE Woods–Saxon single-particle levels, high-spin excitations, lead region nuclei.]

I. INTRODUCTION

Recent interest in nuclear high-spin spectra led to the observation of individual states with spins as high as $I \sim (30-36)\hbar$, thus providing a good basis for testing the quality of the calculated single-particle energy levels. In particular, by investigating the high-spin spectra of nuclei that are expected to preserve their spherical or oblate shapes, as, e.g., some nuclei with Z and N around $Z_0 = 82$ and $N_0 = 126$ or around $Z_0 = 64$ and $N_0 = 82$, one can analyze simultaneously the relative positions of many of the single-particle levels involved in particle-hole excitations, which play a dominant role in the deexcitation schemes of these nuclei. In the $Z_0 = 64$ region, however, a comparison of the calculated and experimental data does not distinguish between effects from single-particle levels and those from residual, as, e.g., pairing, interactions. In this respect the $Z_0 = 82$ region is much cleaner since, due to the presence of large neutron and proton gaps in the single-particle spectra, the pairing Bardeen–Cooper–Schrieffer (BCS) energies Δ_p and Δ_n (solutions to the BCS equations) are zero; consequently, the particle-hole excitations generally do not contain any pairing contributions.

Here, the shell-correction plus particle-hole analysis[1] is used in order to obtain the high-spin excitations. The method is based on the single-particle spectra calculated with the Woods-Saxon potential. The method of generating the potential, which is generally deformed, and solving the corresponding Schrödinger equation is taken from Ref. 2 and thus will not be presented.

The shell-correction plus particle-hole analysis used here does not take into account possible interactions between single-particle and collective degrees of freedom. Consequently, the lowest lying states, close to the characteristic 3^- octupole vibrational states and thus possibly containing admixtures of collective components in their wave functions, are not reproduced well by a pure particle-hole analysis. We thus compare with experiment the relatively high-spin ($I \gtrsim 10\hbar$) excitation energies of ^{212}Rn and ^{204}Pb which are expected to be free from such deficiencies.

In previous studies of high-spin states, both the Nilsson[3] and the Woods–Saxon[4] potential were used. The Nilsson model potential was shown to provide a slightly incorrect single-particle level order in the lead region. In particular, the important $i_{13/2}$ (proton) and $j_{15/2}$ (neutron) levels obtained with the best parameter set had to be rearranged artificially in order to reproduce the experimental level order.[3] Further systematic differences between the Nilsson and Woods–Saxon spectra are discussed in Ref. 4 with respect to high-spin nuclear properties. Calculations based on the Woods–Saxon potential with Rost parameters[5] gave more satisfactory results; but the results for the high-spin spectra of the two nuclei investigated extensively in experiment, ^{212}Rn (Ref. 6) and ^{204}Pb (Ref. 7), can be improved significantly. Calculations making use of the Rost[5] and Chepurnov[8] parameters showed[9] that the former reproduces the ^{212}Rn results slightly better whereas the latter does so for the ^{204}Pb results. Moreover, compared to experiment the average slopes of the calculated yrast lines were not completely satisfactory, although the I^π assignments along the yrast line were basically correct.

The aim of the present investigation is twofold: (i) to provide a uniform set of parameters of the

Woods–Saxon potential which will reproduce the high-spin spectra in the lead region as well as the updated results for the single-particle excitations in this region; and (ii) to compare the calculated single-particle configurations with the shell model results in order to establish the relationship between the shell-model and shell-correction plus particle-hole analysis methods.

II. OPTIMIZATION OF THE WOODS-SAXON POTENTIAL PARAMETERS

The potential is calculated as

$$V(\vec{r};\beta;R_0)=\frac{V_0}{1+\exp[\mathrm{dist}(\vec{r};\beta;r_0)/a]}\,, \tag{1}$$

where $\mathrm{dist}(\vec{r};\beta;r_0)$ is by definition equal to the distance of a point $\vec{r}$ from the nuclear surface Σ defined in terms of quadrupole and hexadecapole deformations, β_2 and β_4, respectively, by

$$\Sigma:\ R(\theta)=R_0c(\beta)[1+\beta_2Y_{20}(\cos\theta)+\beta_4Y_{40}(\cos\theta)]. \tag{2}$$

Here, $\beta\equiv(\beta_2,\beta_4)$; $c(\beta)$ is calculated from the constant volume condition, and $R_0=r_0A^{1/3}$.

The spin-orbit part of the potential was obtained as usually by formula

$$V_{so}=-\lambda\left(\frac{\hbar}{2MC}\right)^2(\vec{\nabla}V|_{r_0\to(r_0)_{so}}\times\vec{P}) \tag{3}$$

in which R_0 was substituted by $R_{so}\equiv(r_0)_{so}A^{1/3}$. Since the single-particle level spectrum, and the level order, depend sensitively on the parameters of the spin-orbit potential, the central part of the potential controlling mainly the number of levels in the potential well, the optimization should be accomplished by choosing its parameters properly.

The parameter optimization was begun by comparing the experimental results for the single-particle energies in ^{208}Pb (Ref. 10 and references cited therein) with the Woods–Saxon potential spectra calculated according to several parametrizations, as proposed in the literature. In this comparison the parameters proposed in Ref. 5 are among the best; we thus attempted the optimization using those parameters as starting values.

In this parametrization the strength λ of the spin-orbit potential for neutrons is characteristically almost twoice as large as that for protons ($\lambda=31.50$ and $\lambda=17.80$ for neutrons and protons, respectively). The $(r_0)_{so}$ neutron and proton parameters also differ significantly [$(r_0)_{so}=1.28$ fm and $(r_0)_{so}=0.93$ fm for neutrons and protons, respectively]. In Chepurnov's parametrization,[8] however, $\lambda=33.87$ and $(r_0)_{so}=1.24$ fm for both neutrons and protons. A relation between the two

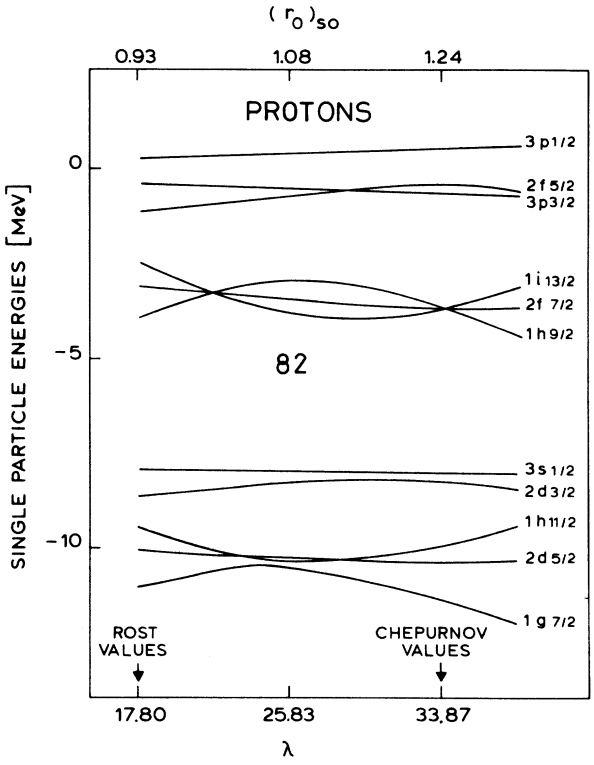

FIG. 1. Single-particle proton levels as functions of the spin-orbit strength parameter λ (lower scale) and the spin-orbit radius parameter $(r_0)_{so}$ (upper scale). All other parameter values are identical with those of Rost. Rost's and Chepurnov's values are explicitly indicated. At $\lambda\approx36.0$ and $(r_0)_{so}\approx1.3$ fm (not displayed) the $2f_{5/2}$ and $3p_{3/2}$ levels will already have crossed, and thus the level order is reestablished.

parametrizations is illustrated in Fig. 1: Starting from the Rost values, the simultaneous increase of λ and $(r_0)_{so}$ causes at the beginning several intersections of levels, but at $\lambda\approx36.0$ and $r_{so}\approx1.3$ fm, i.e., after $2f_{5/2}$ and $3p_{3/2}$ cross again, the single-particle level order is again correct. Simple geometrical considerations lead to the conclusion that decreasing the spin-orbit potential radius parameter with respect to the central potential radius pronounces the role of the former by strongly influencing the slope of the effective potential ($V_{centr}+V_{so}$); increasing the strength parameter λ acts similarly. Consequently, the effects due to relatively drastic changes of λ and $(r_0)_{so}$ (see Fig. 1), when occuring simultaneously, partly cancel each other; one should bear in mind, however, that the overall dependence of single-particle states on the potential parameters is very nonlinear, and thus the above argumentation remains qualitative.

A similar transition from Rost to Chepurnov $[\lambda,(r_0)_{so}]$ parameter values is illustrated in Fig.

2 for neutrons. Now the increase of λ and decrease of $(r_0)_{so}$ complement each other, thus increasing the effect on $(V_{centr}+V_{so})$; the range of parameter variation is much smaller here than in Fig. 1. In both figures Rost values are assumed for all other potential parameters, and thus one should not conclude about the quality of Chepurnov's fit. We expected to reproduce the single-particle level order for neutrons and protons using λ and $(r_0)_{so}$ values common for both kinds of particles. This expectation is supported qualitatively by the results of Fig. 2: The increase of λ from 31.50 to 33.87 to 36.0 can be compensated for by increasing $(r_0)_{so}$ from 1.28 to 1.30 fm. The corresponding calculations are illustrated in Figs. 3 and 4 for protons and neutrons, respectively. In addition to the experimental data given for comparison, the more detailed analysis results of Werner and co-workers,[11] denoted in the figures by "EXP."+CORR, indicate the "real" single-particle levels, i.e., experimental values which were corrected for the fact that a nucleon in the nucleus is subjected to some interaction with its partners. In other words, a single-particle state is excited not only by promoting a particle from its initial to its final level, as calculated from the independent particle model, e.g., the Woods–Saxon model, but also by overcoming the interaction with all other nucleons

$$E_\nu^{sp} = e_\nu^{obs} + \delta e_\nu^{int} . \tag{4}$$

In formula (4) E_ν^{sp} denotes the single-particle energy levels, e_ν^{obs} the corresponding observed quantities which differ[11] from the former by a correction term δe_ν^{int} that accounts for the interaction of a nucleon with the nucleus. Whereas the proton spectrum is not influenced greatly by the correction terms, in the neutron spectrum the most pronounced modification takes place when the distance between the $1i_{11/2}$ and $1j_{15/2}$ levels decreases significantly. Since the choice of $\lambda = 36.0$ and $(r_0)_{so} = 1.3$ fm for both neutrons and protons is in agreement with the discussed empirical data, we accepted it as input for further tests in the high-spin state analysis (all parameter values are collected in Table I).

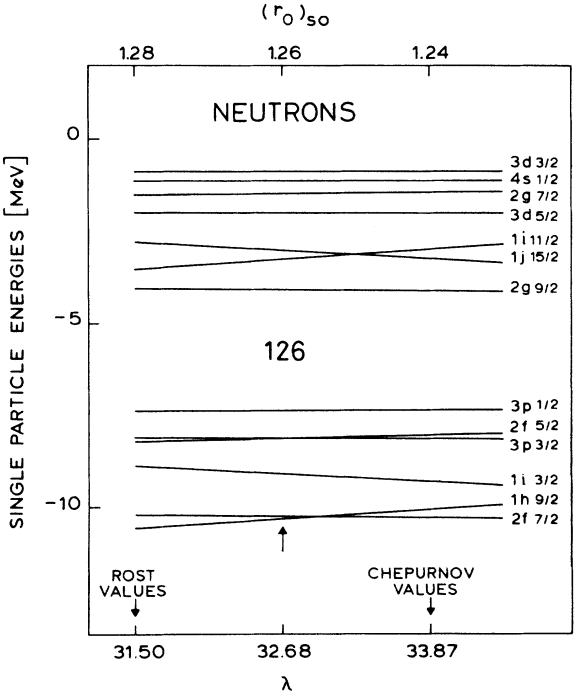

FIG. 2. Single-particle neutron levels as functions of the spin-orbit strength parameter λ (lower scale) and the spin-orbit radius parameter $(r_0)_{so}$ (upper scale). Here, the increase of λ and the decrease of $(r_0)_{so}$ both strengthen the effect of the spin-orbit part of the potential (see also Fig. 4).

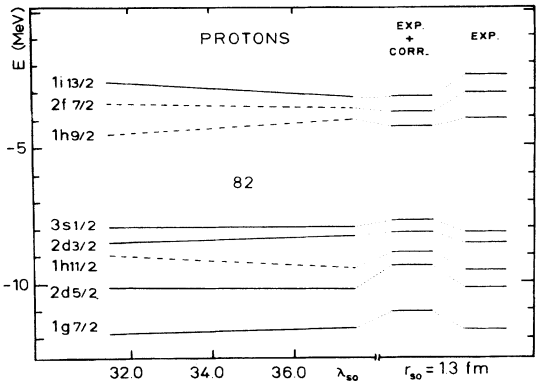

FIG. 3. Single-particle proton levels as functions of the spin-orbit potential strength parameter $(\lambda \equiv \lambda_{so})$ for $(r_0)_{so}$ fixed at 1.3 fm. The experimental values (data from Ref. 10 and references cited therein), denoted by EXP., are corrected for nucleon-nucleus interaction (Ref. 11) (EXP.+CORR).

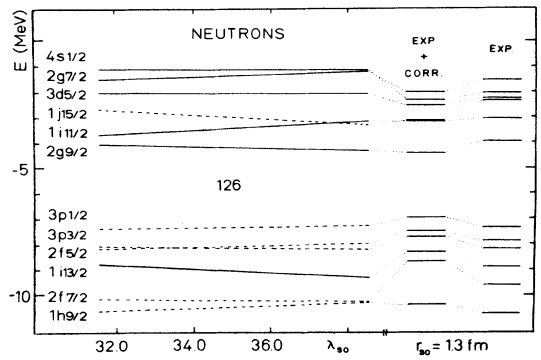

FIG. 4. Single-particle neutron levels as functions of the spin-orbit potential strength parameter $(\lambda \equiv \lambda_{so})$. For further explanations see caption to Fig. 3.

TABLE I. The final parameter values reproducing the single-particle level spectra of ^{208}Pb and high-spin excitations of ^{212}Rn and ^{204}Pb. The parameter $V_0(Z,N) = V[1 \pm \kappa(N-Z)/(N+Z)]$, with the plus sign for protons and the minus sign for neutrons. The Coulomb potential of protons was taken in the form of the classical electrostatic field generated by a uniform charge distribution with the radius equal to $R_c = R_0 = (r_0)_\infty A^{1/2}$. With this parameter choice, discrepancies between the calculated and empirical data (Figs. 3 and 4) generally do not exceed 1 MeV, except for the $2f_{7/2}$ state which, however, lies deeply enough not to be able to influence the high-spin calculation results. Slight changes in V act on the single-particle spectrum, roughly speaking, by shifting the single-particle levels in the energy scale; this property can be used to adjust better the nucleonic binding energies.

	Parameters						
Particles	V (MeV)	κ	r_0 (fm)	a (fm)	λ	$(r_0)_\infty$ (fm)	a_∞ (fm)
Neutrons	−49.6	0.86	1.347	0.70	36.0	1.30	0.70
Protons	−49.6	0.86	1.275	0.70	36.0	1.30	0.70

The high-spin excitations are calculated using the shell-correction plus particle-hole analysis method.[1,4] The total energy is calculated from the relation

$$E(\beta,I) = E_{\mathrm{LD}}(\beta) + \delta E_{\mathrm{shell}}(\beta) + \delta E_{\mathrm{ph}}(\beta,I)\,, \tag{5}$$

with $\delta E_{\mathrm{shell}}$ calculated from the Strutinsky method and

$$\delta E_{\mathrm{ph}}(\beta,I) = \sum_{p\in\{p\}} e_p - \sum_{h\in\{h\}} e_h\,, \tag{6}$$

where $\{p\}$ and $\{h\}$ denote the set of particle and hole states, respectively. The quantity $E_{\mathrm{LD}}(\beta)$ represents the liquid drop model energy with the parameters taken from Myers and Swiatecki[12]; in the Strutinsky type calculations the smoothing parameter γ was equal to $1.2 \times (41/A^{1/3})$ MeV, and the highest order p of the smoothing polynomial was set equal to 6 (for details see Refs. 13 and 14).

In the high-spin calculations the proton and neutron particle-hole excitation energies were generated first at the deformations $\beta_2 = 0, -0.04, -0.08, -0.012, -0.16$ ($\beta_4 = 0$). Then the proton and neutron contributions at a given deformation were added up and the sequence of a few lowest energy states for a given spin I ($0 \leq I/\hbar \leq 50$) was found. Finally, the yrast energies were calculated as those realizing a minimum with respect to the deformation.

The results of these calculations are presented in Figs. 5 and 6 for ^{204}Pb and ^{212}Rn, respectively. Since this method does not take into account any coupling with collective degrees of freedom, we arbitrarily normalized the experimental and theoretical spectra to zero at $I^\pi = 9^-$ for ^{204}Pb and $I^\pi = 12^+$ for ^{212}Rn. The proposed set of parameters (Table I) offers a good description of the high-spin states in ^{204}Pb; as usual, the calculations predict some yrast states which were not yet observed experimentally.

The calculated high-spin states of ^{212}Rn are compared in Fig. 6 with the experimental ones and with analogous results of calculations based on the shell model.[15] The spherical shell model results[15] generally agree with experiment very well for spin values which are not too high. On the other hand, the shell model employs a number of adjustable parameters that are taken from a com-

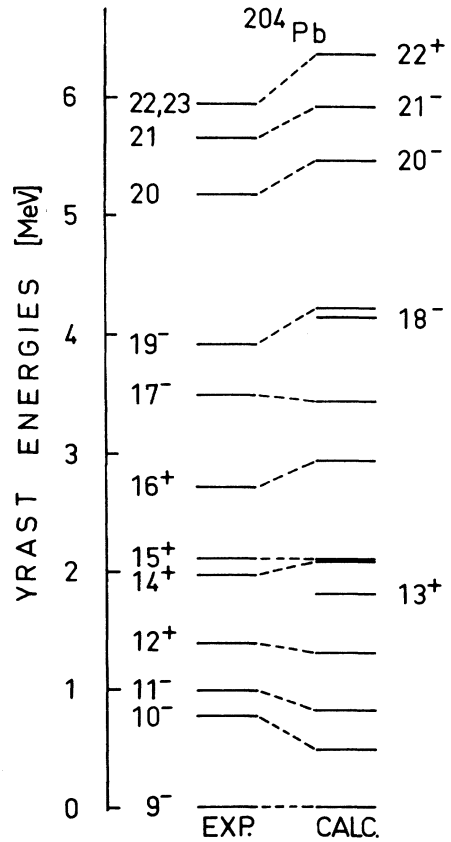

FIG. 5. Yrast energies of ^{204}Pb (experimental data from Ref. 7). The calculated results correspond to optimized parameters (Table I).

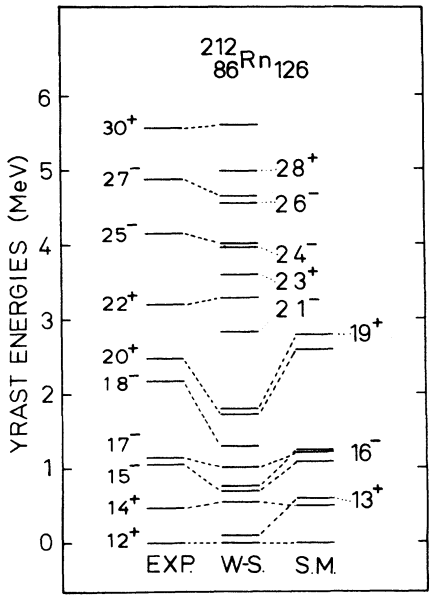

FIG. 6. Yrast energies of ^{212}Rn (experimental data from Ref. 6). The shell-correction plus particle-hole analysis results based on the Woods–Saxon single-particle levels with the parameters from Table I are denoted by WS. For comparison, the shell model results of Ref. 15 (S.M.) are also shown.

parison of spectra of several nuclei from the neighborhood of the investigated one. The shell-correction plus particle-hole analysis, however, can easily be extended to deformed (oblate) shapes and to very high spin excitations, the latter being rather difficult to achieve within the shell model methods due to the fast increase of dimensions of the matrices involved.

It is also interesting to compare the calculated single-particle structure of the high spin states as calculated with the two approaches (Table II; see also Ref. 16 for further details). In fact, for such a comparison it was sufficient to display the results of only one method, since both the shell-correction plus particle-hole analysis and the shell model results[15] predict identical configurations. The results of the former approach are presented in Tables II and III.

The deformation resulting from these calculations is weak but significant: For the lowest spin states it is close to zero and decreases, with negative quadrupole deformation signifying oblate shapes, to $\beta_2 \approx (-0.08, -0.10)$ for the highest spin states considered.

III. SUMMARY AND CONCLUSIONS

The knowledge of high-spin excitations in spherical or oblate nuclei allows us to examine the single-particle nucleon spectra in addition to the traditional one- or two-particle transfer reaction methods. We employed the high-spin excitation and particle transfer reaction data to deduce the best Woods–Saxon potential parameter values for the nuclei of the lead region.

The proposed parameter set reproduces well the experimental data. The spin-orbit potential parameters obtained are identical for both neu-

TABLE II. Configurations of the excited high-spin states of ^{212}Rn. All the configurations for $I \leq 20\hbar$ agree with those of Ref. 15 (higher spin states were not analyzed in Ref. 15). Our configurations of the 25^-, 27^-, and 30^+ states agree with those obtained in Ref. 17 rather than with those proposed in Ref. 6.

I^π	Protons	Neutrons
12^+	$h_{9/2}{}^4$	
13^+	$h_{9/2}{}^3, f_{7/2}$	
14^+	$h_{9/2}{}^3, f_{7/2}$	
15^-	$h_{9/2}{}^3, i_{13/2}$	
16^-	$h_{9/2}{}^3, i_{13/2}$	
17^-	$h_{9/2}{}^3, i_{13/2}$	
18^-	$h_{9/2}{}^2, f_{7/2}, i_{13/2}$	
19^+	$h_{9/2}{}^2, i_{13/2}{}^2$	
20^+	$h_{9/2}{}^2, i_{13/2}{}^2$	
21^-	$h_{9/2}, i_{13/2}{}^3$	
22^+	$h_{9/2}{}^3, i_{13/2}$	$p_{1/2}{}^{-1}, g_{9/2}$
23^+	$h_{9/2}{}^2, i_{13/2}, f_{7/2}$	$p_{1/2}{}^{-1}, g_{9/2}$
24^-	$h_{9/2}{}^2, i_{13/2}{}^2$	$p_{1/2}{}^{-1}, g_{9/2}$
25^-	$h_{9/2}{}^2, i_{13/2}{}^2$	$p_{1/2}{}^{-1}, g_{9/2}$
26^-	$h_{9/2}{}^2, i_{13/2}, f_{7/2}$	$p_{1/2}{}^{-1}, j_{15/2}$
27^-	$h_{9/2}{}^2, i_{13/2}{}^2$	$p_{1/2}{}^{-1}, j_{15/2}$
28^+	$h_{9/2}{}^2, i_{13/2}{}^2$	$p_{1/2}{}^{-1}, j_{15/2}$
29^+	$h_{9/2}{}^2, i_{13/2}{}^2$	$f_{5/2}{}^{-1}, j_{15/2}$
30^+	$h_{9/2}{}^2, i_{13/2}, f_{7/2}$	$p_{1/2}{}^{-2}, g_{9/2}, j_{15/2}$

TABLE III. Configurations of the excited high-spin states of ^{204}Pb. According to the interpretation proposed in Tables II and III the $I \leq 20\hbar$ states of ^{204}Pb presumably test the neutron configurations, while the $I \leq 22\hbar$ states of ^{212}Rn presumably test the proton configurations.

I^π	Protons	Neutrons
9^-		$f_{5/2}{}^{-1}, i_{13/2}{}^{-1}, f_{5/2}{}^2$
10^-		$f_{5/2}{}^{-1}, i_{13/2}{}^{-1}, f_{5/2}, p_{1/2}$
11^-		$f_{5/2}{}^{-1}, i_{13/2}{}^{-1}, f_{5/2}, p_{1/2}$
12^+		$i_{13/2}{}^{-2}, f_{5/2}{}^2$
13^+		$i_{13/2}{}^{-2}, f_{5/2}, p_{1/2}$
14^+		$f_{5/2}{}^{-1}, i_{13/2}{}^{-2}, f_{5/2}{}^2, p_{1/2}$
15^+		$f_{5/2}{}^{-1}, i_{13/2}{}^{-2}, f_{5/2}{}^2, p_{1/2}$
16^+		$f_{5/2}{}^{-2}, i_{13/2}{}^{-2}, f_{5/2}{}^2, p_{1/2}$
17^-		$i_{13/2}{}^{-3}, f_{5/2}{}^2, p_{1/2}$
18^-		$f_{5/2}{}^{-1}, i_{13/2}{}^3, f_{5/2}{}^2, p_{1/2}{}^2$
19^-		$f_{5/2}{}^{-1}, i_{13/2}{}^3, f_{5/2}{}^2, p_{1/2}$
20^-	$h_{11/2}{}^{-1}, h_{9/2}$	$f_{5/2}{}^{-2}, i_{13/2}{}^{-1}, f_{5/2}{}^2, p_{1/2}$
21^-	$h_{11/2}{}^{-1}, h_{9/2}$	$f_{5/2}{}^{-2}, i_{13/2}{}^{-1}, f_{5/2}{}^2, p_{1/2}$
22^+		$f_{5/2}{}^{-1}, i_{13/2}{}^{-2}, f_{5/2}{}^2, j_{15/2}$

trons and protons; all other parameters are taken from Rost[5] (the final parameter values are collected in Table I).

The resulting single-particle configurations of the ^{212}Rn high-spin states are compared with the shell model calculation results; both methods are shown to interpret the structure of yrast states identically. This is considered to be evidence for the validity of the shell-correction plus particle-hole analysis method which, in contrast to the spherical shell model, can easily be extended to very high spins and large oblate deformations.

[1]G. Andersson, S. E. Larsson, G. Leander, P. Möller, S. G. Nilsson, I. Ragnarsson, S. Aberg, R. Bengtsson, J. Dudek, B. Nerlo-Pomorska, K. Pomorski, and Z. Szymański, Nucl. Phys. A268, 205 (1976).
[2]J. Dudek, A. Majhofer, J. Skalski, T. Werner, S. Cwiok, and W. Nazarewicz, J. Phys. G 5, 1359 (1979).
[3]C. G. Andersson, G. Hellström, G. Leander, I. Ragnarsson, S. Aberg, J. Krumlinde, S. G. Nilsson, and Z. Szymański, Nucl. Phys. A309, 141 (1978).
[4]M. Cerkaski, J. Dudek, Z. Szymański, P. Rozmej, and S. G. Nilsson, Nucl. Phys. A315, 269 (1979).
[5]E. Rost, Phys. Lett. 26B, 184 (1968).
[6]D. Horn, O. Hausser, T. Faestermann, A. B. McDonald, T. K. Alexander, J. R. Beene, and C. J. Herrlander, Phys. Rev. Lett. 39, 389 (1977).
[7]C. G. Linder, I. Bergström, J. Blomqvist, and C. Roulet, annual report, 1974, Research Institute for Physics, Stockholm, p. 117; Z. Phys. A 284, 217 (1978).
[8]V. A. Chepurnov, Yad. Fiz. 5, 955 (1967) [Sov. J. Nucl. Phys. 6, 696 (1968)].
[9]J. Dudek and T. Werner, unpublished.
[10]A. Bohr and B. R. Mottelson, *Nuclear Structure* (Benjamin, New York, 1969), Vol. I.
[11]R. Werner, K. Dietrich, P. Møller, and J. R. Nix, in *Proceedings of the Fourth IAEA Symposium on the Physics and Chemistry of Fission, Jülich, 1979* (IAEA, Vienna, 1980).
[12]W. D. Myers and W. Swiatecki, Ark. Fys. 36, 593 (1967).
[13]V. M. Strutinsky, Nucl. Phys. A95, 420 (1967).
[14]M. Bolsterli, E. O. Fiset, J. R. Nix, and J. L. Norton, Phys. Rev. C 5, 1050 (1972).
[15]J. Blomqvist, Proceedings of the International Conference on High Spin Phenomena, Argonne, 1979.
[16]J. Dudek, International Conference on Nuclear Behavior at High Angular Momenta, Strasbourg, 1980.
[17]K. Matsuyanagi, T. Døssing, and K. Neergaard, Nucl. Phys. A307, 253 (1978).